

**Zeitschrift:** IABSE reports = Rapports AIPC = IVBH Berichte  
**Band:** 62 (1991)

**Rubrik:** Punching of slabs

### **Nutzungsbedingungen**

Die ETH-Bibliothek ist die Anbieterin der digitalisierten Zeitschriften. Sie besitzt keine Urheberrechte an den Zeitschriften und ist nicht verantwortlich für deren Inhalte. Die Rechte liegen in der Regel bei den Herausgebern beziehungsweise den externen Rechteinhabern. [Siehe Rechtliche Hinweise.](#)

### **Conditions d'utilisation**

L'ETH Library est le fournisseur des revues numérisées. Elle ne détient aucun droit d'auteur sur les revues et n'est pas responsable de leur contenu. En règle générale, les droits sont détenus par les éditeurs ou les détenteurs de droits externes. [Voir Informations légales.](#)

### **Terms of use**

The ETH Library is the provider of the digitised journals. It does not own any copyrights to the journals and is not responsible for their content. The rights usually lie with the publishers or the external rights holders. [See Legal notice.](#)

**Download PDF:** 23.11.2024

**ETH-Bibliothek Zürich, E-Periodica, <https://www.e-periodica.ch>**

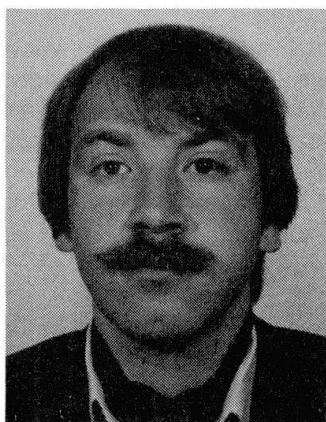
## Behaviour of Beams and Punching in Slabs without Shear Reinforcement

Comportement des poutres et poinçonnement des dalles  
sans armatures d'effort tranchant

Tragverhalten von Balken und Durchstanzen von Platten  
ohne Schubbewehrung

### Aurelio MUTTONI

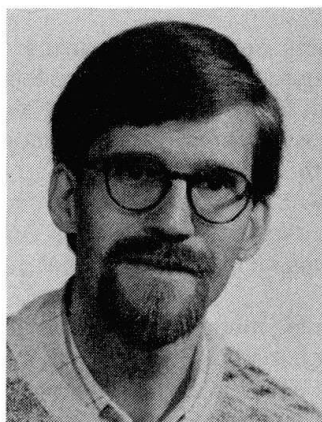
Dr. sc. techn.  
Grignoli, Martinola, Muttoni  
Lugano, Switzerland



Aurelio Muttoni graduated in Civil Engineering at the Swiss Federal Institute of Technology in 1982 and subsequently undertook research on the applicability of the theory of plasticity to the design of reinforced concrete structures, obtaining his Ph.D. degree in 1989.

### Joseph SCHWARTZ

Dr. sc. techn.  
Frey, Consult. Eng.  
Zug, Switzerland



Joseph Schwartz graduated in Civil Engineering at the Swiss Federal Institute of Technology in 1981 and subsequently undertook research on the stability of masonry and reinforced concrete members, obtaining his Ph.D. degree in 1989.

### SUMMARY

The cause of shear failure is investigated in beams and slabs without shear reinforcement. The main parameters influencing the structural behaviour are discussed. A theoretical model for the determination of the punching strength as a function of different parameters including size effect is proposed.

### RÉSUMÉ

On analyse ici la cause de la rupture par cisaillement des poutres et des dalles sans armature d'effort tranchant. Un modèle théorique visant la détermination de la résistance au poinçonnement est proposé en traction de différents paramètres dont l'effet de taille.

### ZUSAMMENFASSUNG

Die Ursache des Schubbruches von Balken und Platten ohne Schubbewehrung wird untersucht. Die Hauptparameter, welche das Tragverhalten beeinflussen, werden diskutiert. Ein theoretisches Modell zur Berechnung des Durchstanzwiderstandes in Funktion verschiedener Parameter einschliesslich «size effect» wird vorgeschlagen.



## 1. SHEAR ACTION IN BEAMS WITHOUT SHEAR REINFORCEMENT

The investigation begins with the consideration of the simple beam shown in Fig. 1. The reinforcement consists of longitudinal bars, which are completely anchored behind the supports. Not taking into account the tensile strength of the concrete and without shear reinforcement (stirrups) the only possible structural model is the so-called direct support, i.e. between the load and the reaction force a compression zone resembling a concrete strut is formed. The stress field proposed by Drucker [1] to describe this load bearing action is shown in Fig. 2. It is the solution according to plasticity theory.

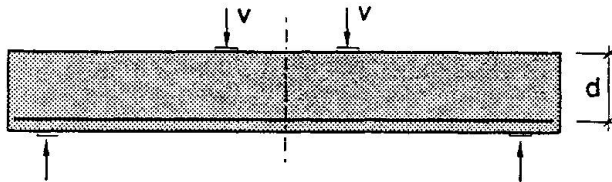


Fig. 1 Beam and loading

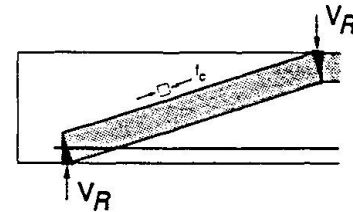


Fig. 2 Stress field

This stress field can under some circumstances deviate greatly from the actual structural action. While increasing the load  $V$  monotonically from zero to the level of the failure load  $V_R$  several phases of load bearing action may be recognized. After cracks due to bending develop, the load bearing action begins to deviate from that of the elastic model which presupposes homogeneous behaviour. If one assumes that there is no load transfer over the cracks then the new internal load bearing action can be described by the stress resultants shown in Fig. 3b. This load bearing model was already recognized by Kani [2] and described as follows: "Due to the transverse cracks the tension zone is divided up into separate concrete elements, which can be visualized as cantilever beams fixed in the upper compression zone".

Further possible load bearing models are sketched together with the stress resultants in Figs. 3c and 3d. In the case of the structural model shown in Fig. 3c concrete compressive forces are assumed to be transferred across the cracks. This is possible as the roughness of the cracked surface causes an interlocking behaviour. Fig. 3d shows a structural model in which the longitudinal reinforcement also transmits forces in the transverse direction (so-called dowelling action). The effective stress field results from the combination of the three load bearing models mentioned, as also Hamadi and Regan [3], Reineck [4] and others have shown.

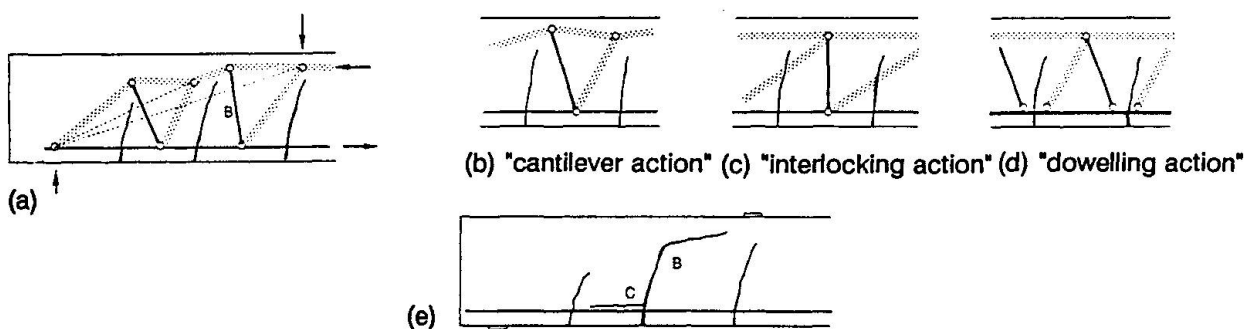


Fig. 3 Structural models after bending cracks develop with subsequent crack propagation

If the load is increased further the tensile strength is reached in region B (Fig. 3a). The original bending crack running almost vertical then propagates in a more or less horizontal direction. A typical crack pattern is shown in Fig. 3e. The propagation of this crack is accompanied by a collapse of the three abovementioned structural models. The cantilever and interlocking models lose their load bearing capacity because the concrete ties at B are broken. The dowelling action also becomes ineffective because a crack forms at C (Fig. 3e).

The new structural model, which could now become effective, is the plasticity solution already mentioned, i.e. the direct support model. Fig. 4a shows the crack pattern just prior to failure in a beam tested at the Institute of Structural Engineering at the Swiss Federal Institute of Technology, Zurich [5]. In this figure the stress field describing the direct support model has been introduced. The dimension of the strut has been determined

from considerations of equilibrium and full exploitation of the concrete strength  $f_c$ . It is clear that the main crack passes through the theoretical strut. The possibility of force transfer across the crack depends on the relative displacements of the crack boundaries and the roughness of the crack surface. The relative displacement vectors measured during the test are shown in Fig. 4b for two load steps  $V = 0.87 \cdot V_R$  and  $V = 0.95 \cdot V_R$ . These displacements may be compared with the relationships between crack opening  $u$  and movement along crack  $v$  given in Fig. 4c. The curves represent the displacement vectors at which contact between the two crack boundaries is just no longer possible and thus force transfer ceases. They were measured on specimens, which were broken into two parts after being cut out of the test beam. A comparison of the two figures shows that practically no more force had been transferred over the crack in the test beam.

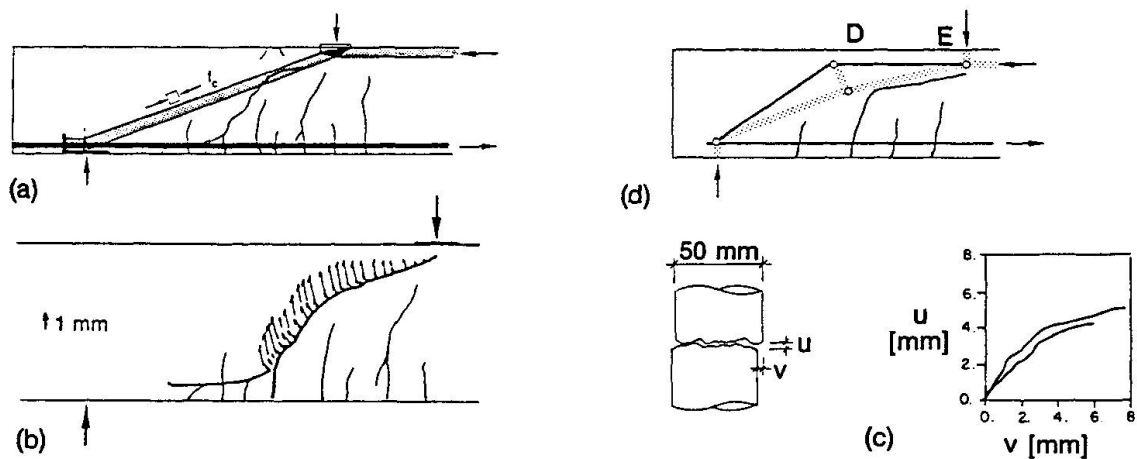


Fig. 4 Structural model; relative displacement of the critical crack

Therefore a stress field with a concrete strut running directly between the load and the support reaction is not possible. Such a strut is only admissible if it is deviated in the central region (Fig. 4d). The concrete strut acts together with a concrete tie, that also exhibits a deviation in the central part of the beam, so that the deviation forces can balance each other out. Failure occurs because the tensile strength in the region D is reached or because the strength in zone E, which is subjected to both tension and compression, is exceeded. Overstressing in this zone can be caused by the crack which propagates to the zone where the load is applied.

It may be easily seen that the load capacity of the stress field (with a bent strut) shown in Fig. 4d is smaller than that given by the plasticity theory (with a straight strut). Therefore the failure load is very dependent upon the crack pattern. Thus there results, especially for tests on small beams, a big scatter in the experimentally determined failure loads. Since the crack pattern depends on the initial state of stress and the load history, the failure load is also influenced by these factors. For this reason a theoretical estimate of the failure load is always encumbered by great difficulties and uncertainties. The position of the critical crack and thus the load capacity depends greatly on a number of parameters, for example slenderness of beam, geometry and axial force. These influences are described in [6].

The correlation between crack pattern and failure load indicates the possibility of improving the structural performance and increasing the failure load by favourably influencing the crack pattern by means of constructional measures. The zone where the strut corresponding to direct support should be formed can for example be kept free of cracks by prestressing the beam such that the load is supported directly from the beginning. This explains why prestressed beams exhibit a greater shear resistance than non-prestressed reinforced beams. A similar improvement in performance is evident when the reinforcement in the region subjected to shear action is not bonded to the concrete. Fig. 5 shows the crack patterns and the stress fields for two tests which differ only in the quality of the bonding. For beams having bond-free reinforcement or with a poor quality of bonding cracks form in the central part. As shown in Fig 5b the inclined strut is hardly affected by these cracks, so that the failure load can be as much as twice that of beams with good bonding quality (Fig. 5a). A further increase of the failure load can be achieved by placing reinforcement in the critical region. Fig. 6 shows the arrangement of reinforcement and the crack pattern at failure of a test reported by Muttoni and Thürlimann [6]. Wide cracks were only obtained in the unreinforced region, which allowed the direct support system to develop. As a result the load could be increased up to the point of yielding of the



longitudinal bars. The failure load was about double that of a similar beam which did not have reinforcement in the region of the concrete strut (Fig. 4a).

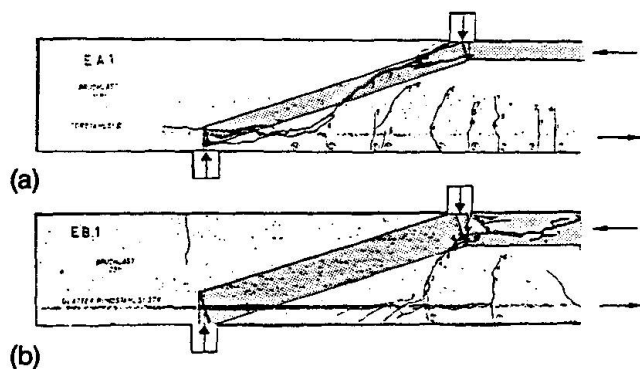


Fig. 5 Influence of bonding

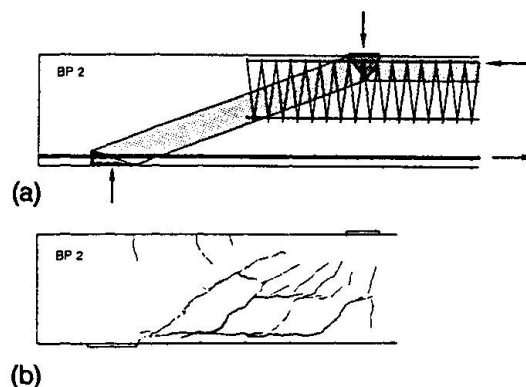


Fig. 6 Influence of reinforcement in the critical zone

## 2. PUNCHING SHEAR

With only small modifications the considerations concerning the internal structural behaviour of beams may be applied to the slab element shown in Fig. 7. Fig 8a shows the position of the stress resultants after tangential cracks have developed.

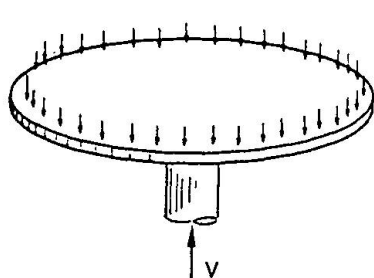


Fig. 7 Slab specimen

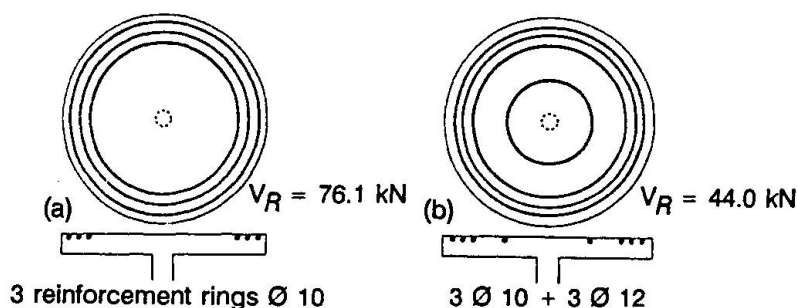


Fig. 9 Punching shear tests with ring reinforcement

As numerous punching shear tests have shown the curvatures in the radial direction are concentrated in the region of the columns, so that ring-shaped concentric bending cracks are only obtained in this region. In the other zones, however, only radial cracks are present. Since shear force is not transferred in the tangential direction, the stress state is not influenced by these cracks. In the region of tangential cracking a part of the shear force can be resisted by the interlocking action at the crack boundaries and by the dowelling action of the reinforcing bars (see Fig. 3). From Fig. 8a it is evident that the horizontal components of the compression and tension diagonals can be resisted by the reinforcement in the radial direction, by the radial compression zone and also by the deviation of the tangentially directed forces in the reinforcement and in the compression zone. On increasing the load the strength of the concrete tie is reached at A, so that the bending crack is propagated in the horizontal direction. The structural action that then results is similar to that obtained in the beam. As no force can be transferred across the crack a bent strut is formed with a tie that is also bent (Fig. 8b).

It has been shown experimentally that often the concrete compression in the radial direction in the compression zone near the column (point B) initially increases under monotonically increasing load and after reaching a certain load level begins to decrease until shortly before failure negative values may be exhibited. This observation is in agreement with the proposed model. The compression decreases once the main bending crack has propagated and its negative value (tensile strain) indicates that at B a tie has formed. Since the structural behaviour and the failure mechanisms are analogous to the those of the beam, for slabs also the same constructional solutions may in principle be employed. The crack pattern can be favourably influenced by omitting reinforcement in the region of the columns. As in the case of beams having reinforcement without

stirrups, whereby cracks can only develop in the vicinity of load application, for such a slab tangential cracks can only develop above the edge of the column. This kind of behaviour has been observed by Bollinger [7] in tests carried out on slab elements. The test shown in Fig 9a was reinforced with concentric rings placed at the boundary of the slab only. The punching shear force for this test was consistently higher than that for similar slabs which also had reinforcement in the region of the column. For the test shown in Fig. 9b the additional reinforcing ring in the critical region (greater amount of reinforcement) even caused a substantial reduction in the punching shear force.

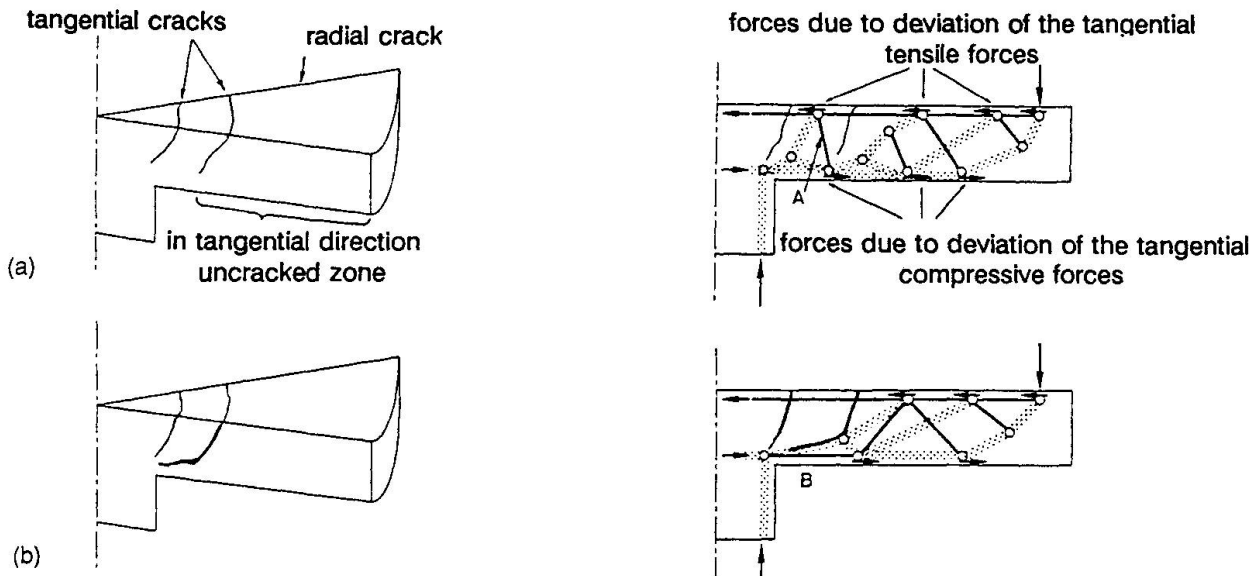


Fig. 8 Structural behaviour in the cracked state

Since in general the critical crack is responsible for the reduction in the failure load the punching shear force is inversely proportional to the width of crack. This is confirmed in Fig.10 in which the load is given as a function of the rotation  $\phi$  in the region of the column for four slabs with different amounts of reinforcement.

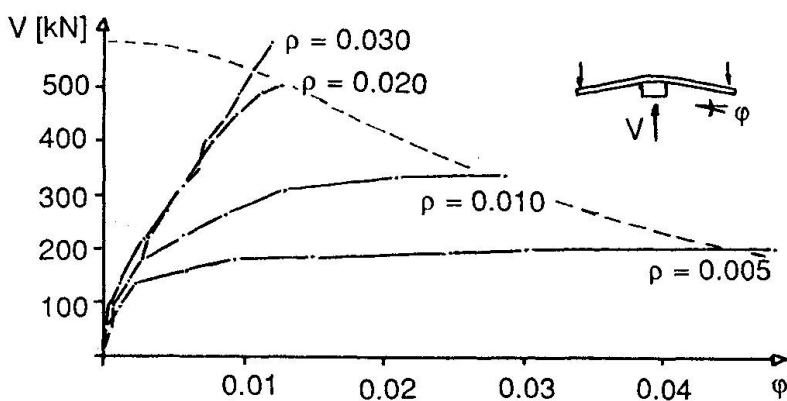


Fig. 10 Load-displacement diagrams of slabs

Since for the four slabs the thickness was kept constant the crack width is also proportional to the rotation  $\phi$ . In Fig. 11a the punching shear forces and the corresponding deformations are shown for further test specimens. Since the crack width inside the slab is a direct function of the slab thickness, for this figure the product of rotation  $\phi$  times statical depth  $d$  was chosen for the abscissa. The ordinate represents normalized nominal punching shear strength. The relationship between punching shear resistance and deformation is described satisfactorily by the curve given in Fig. 10. Good agreement with test results is also obtained when the slab thickness  $h$  alone is varied (Fig. 11b).

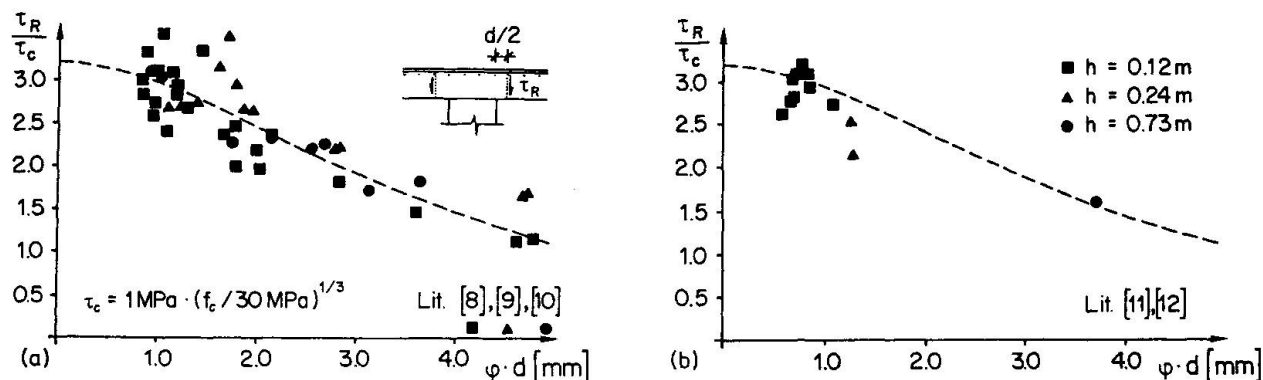


Fig. 11 Nominal punching shear strength in function of  $\phi \cdot d$

With the empirically determined curve for describing the ductility restrictions for axisymmetric slabs the punching shear force can be found analytically.

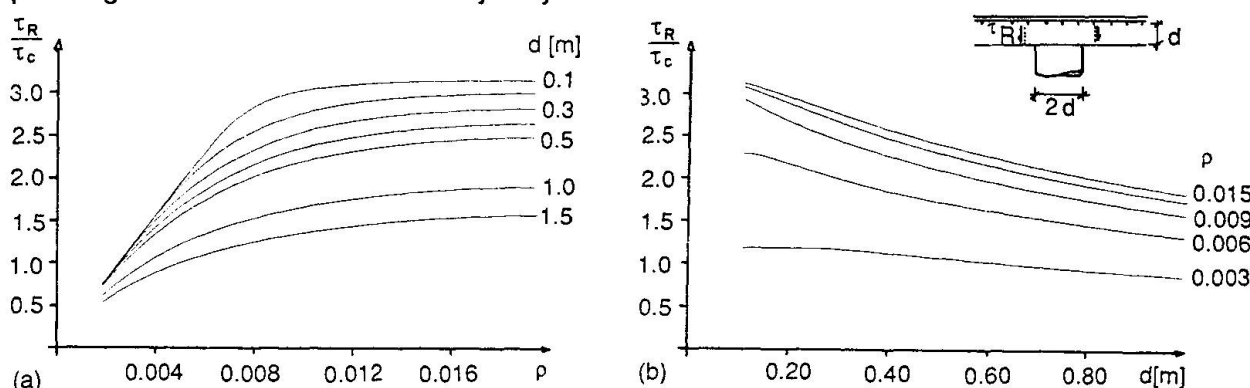


Fig. 12 Nominal punching shear strength in function of amount of reinforcement and slab thickness

From Fig. 12 it is evident that with increasing slab thickness a considerable reduction in punching shear resistance may result, i.e. the geometry or size-effect is important.

## REFERENCES

1. DRUCKER D.C., On Structural Concrete and the Theorems of Limit Analysis. Internat. Association for Bridge and Structural Engineering, Zurich, IABSE-Reports 21, 1961.
2. KANI G., Spannbeton in Entwurf und Ausführung. Konrad Wittwer Publishers, Stuttgart, 1955.
3. HAMADI Y.D., REGAN P.E., Behaviour in Shear of Beams with Flexural Cracks. Magazine of Concrete Research, Vol. 32, No. 111, June, 1980.
4. REINECK K.-H., Models for Design of Reinforced and Prestressed Concrete Members. Comité Euro-International du Béton (CEB), Bulletin d'information No. 146/1982.
5. MUTTONI A., THÜRLIMANN B., Schubversuche an Balken und Flachdecken ohne Schubbewehrung. Institute of Structural Engineering, ETH Zurich, 1986, unpublished report.
6. MUTTONI A., Die Anwendbarkeit der Plastizitätstheorie in der Bemessung von Stahlbeton. ETH Zurich, IBK, Report Nr. 176 (Ph.D. Thesis), Birkhäuser Verlag, Basel, 1990.
7. BOLLINGER K., Zu Tragverhalten und Bewehrung von rotationssymmetrisch beanspruchten Stahlbetonplatten. University of Dortmund (Ph.D. Thesis), 1985.
8. ELSTNER R.C., HOGNESTAD E., Shearing Strength of R.C. Slabs. ACI Journal, July, 1956.
9. KINNUNEN S., NYLANDER H., Punching of Concrete Slabs without Shear Reinforcement. Kungl. Tekniska Högskolans Handlingar, Stockholm, Report No. 158, 1960.
10. TOLF, P., Planiöcklekens inverkan på betongplattors hallfasthet vid genomstansning. Kungl. Tekniska Högskolans, Stockholm, Meddelande No. 146, 1988.
11. NYLANDER H., SUNDQUIST H., Genomstansning av pelarunderstödd plattbro av betong med ospänd armering. Meddelande 104, Kungl. Tekniska Högskolan, Stockholm, 1972.
12. KINNUNEN S., NYLANDER H., TOLF P., Plattjöcklekens inverkan på betongplattors hallfasthet vid genomstansning. Försök med rektangulära plattor. M. 137, Kungl. Tekn. Högskolan, Stockholm, 1980.

## **Bond Model for Punching Strength of Slab-Column Connections**

**Modèle de liaison pour résistance au poinçonnement dans les têtes  
de colonnes en béton armé**

**Physikalisches Modell für das Durchstanzen von Flachdecken**

### **Scott D. B. ALEXANDER**

Univ. of Alberta  
Edmonton, AB, Canada

### **Sidney H. SIMMONDS**

Univ. of Alberta  
Edmonton, AB, Canada

Scott Alexander recently completed his Ph.D. in civil engineering at the University of Alberta. He is currently a research engineer with the Network of Centres of Excellence on High Performance Concrete.

Sidney Simmonds received his Ph.D. in civil engineering at the University of Illinois in 1962. His research has been primarily in the area of design and behaviour of reinforced concrete structures and he is a member of a number of related technical committees.

### **SUMMARY**

A physical model that explains the mechanism of punching failure in reinforced concrete column-flat plate connections is presented. Load is carried to the column face by arching action in the radial direction. The curvature of the arch is defined by the force gradient (bond) that can be developed in the reinforcement perpendicular to the arch. The validity of the model is demonstrated by comparing predicted capacities with results from tests of such connections.

### **RÉSUMÉ**

Un modèle physique est présenté qui explique le mécanisme de rupture par poinçonnement dans les têtes de colonnes en béton armé, au droit de leur connexion avec une dalle. La charge est transmise au bord de la colonne de façon radiale, sous forme d'une action légèrement arquée. La courbure de cet arc est définie par le gradient de forces pouvant se développer dans l'armature qui se trouve perpendiculaire à l'arc. La validité de ce modèle est démontrée par la comparaison des capacités prévues de résistance, illustrée par les résultats d'essais effectués sur de tels systèmes de connexion.

### **ZUSAMMENFASSUNG**

Es wird ein physikalisches Modell für das Durchstanzen von Flachdecken vorgestellt. Die Last wird über eine radiale Bogentragwirkung zum Stützenkopf übertragen. Die Bogenform wird durch den Abbau des Verbundes in der Ringbewehrung bestimmt. Die Gültigkeit des Modells wird durch den Vergleich mit Bruchversuchen bestätigt.





## 1 Introduction

The truss model<sup>1</sup> describes a slab-column connection as a space truss composed of steel tension ties and straight-line concrete compression struts. Although this model provides an excellent qualitative description for the behavior of slab-column connections, the location of the intersection between the effective centroid of the strut and the top mat reinforcing steel does not agree with the position of the strut as determined from measured bar force profiles at failure<sup>2</sup>. A model that retains the desirable characteristics of the truss model and is consistent with experimental measurements of strain is required.

A curved arch, as shown in Fig. 1, is consistent with measured bar force profiles. In plan, the arch is parallel to the reinforcement. As with the truss model, the horizontal component of the arch is equilibrated by tension in the reinforcement. By limiting the width of the arch to the width of the column support, the arch may be considered a purely radial component within the plate, thereby preserving the truss model concept of shear being carried radially by an inclined concrete compression strut. The geometry of the curved radial arch, however, cannot be determined from the bar force profile of the reinforcement tying the arch.

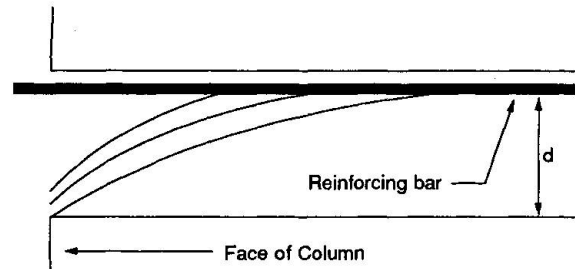


Fig. 1: Radial Arch

If the horizontal force component in the arch is assumed to be constant, then the shear carried by the arch varies from a maximum at the face of the column where the slope of the arch is large to a minimum, or perhaps zero, at the intersection of the arch and the reinforcing steel where the slope is small. The shear that was carried by the arch at the face of the column must be dissipated in a direction perpendicular to the arch at some distance away from the column. The rate at which shear can be dissipated determines the curvature of the arch.

In a reinforced concrete flexural member, moment is calculated as the product of the steel force,  $T$ , and an effective moment arm,  $jd$ . Moment gradient or shear results wherever the magnitude of the force or moment arm varies along the length of the member ( $x$ -axis).

$$V = \frac{d(Tjd)}{dx} = \frac{d(T)}{dx}jd + \frac{d(jd)}{dx}T \quad [1]$$

Shear that is the result of a gradient in tensile force acting on a constant moment arm is carried by **beam action**. Shear resulting from a constant tensile force acting on a varying moment arm is carried by **arching action**. Whereas beam action at a particular cross-section requires bond forces at that cross-section, arching action requires only remote anchorage of the reinforcement.

Experimental observations suggest that beam action is the only possible mechanism of shear transfer in what amounts to a circumferential direction. For example, Kinnunen and Nylander<sup>3</sup>, report that the deformed shape of test specimens under load is essentially conic, with little or no curvature in the radial direction. This requires a linear distribution of circumferential strain through the thickness of the plate, with maximum compressive strain at the slab soffit. This means that the flexural depth,  $jd$ , in the circumferential direction is relatively constant, and any shear carried in the circumferential direction must be carried by the two-way plate equivalent of beam action.

Beam action shear requires a force gradient in the reinforcement. Force gradient may be limited by either yielding of the reinforcement or by bond failure. For those connections that fail prior to widespread yielding, bond strength is the most important limitation on force gradient, hence, the term **bond model**.

## 2 Development of Bond Model

The orthogonally reinforced slab-column connection is modelled as a rectangular grillage, as shown in Fig. 2. Four strips, called radial strips, extend from the column parallel to the reinforcement. Any load reaching the column must pass through one of these four radial strips. The width of each strip is defined by the column width. The end of the strip farthest from the column support, called

the remote end, is placed at a position of zero shear. Thus, radial strips are loaded in shear on their side faces only. The total length of a strip is designated as  $L$ . The strength of the connection is determined by assessing both the flexural strength of each radial strip and the ability of the adjacent quadrants of two-way plate to load each radial strip.

Consider the free body diagram of one-half of a radial strip shown in Fig. 3. The half-strip must support the combined effect of any load applied directly to the strip ( $q$ ), including the self-weight of the strip, and the internal shears and moments developed on the side faces of the strip by the adjacent quadrants of two-way plate. The near side face of the half-strip is loaded in shear ( $v$ ), torsion ( $m_t$ ) and bending ( $m_n$ ) by the adjacent quadrant of two-way plate. The far side face lies on an axis of symmetry for the plate. Under concentric loading, both shear and torsion on this face are zero. The bending moment applied to the far side face of the half-strip is equal and opposite to the bending moment on the near side face.

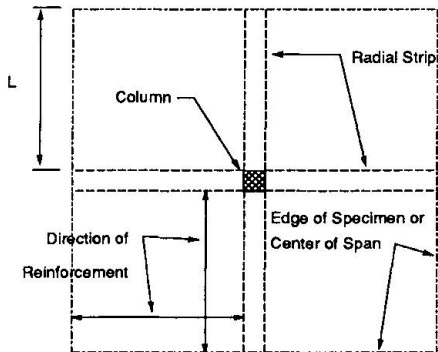


Fig. 2: Layout of Radial Strips

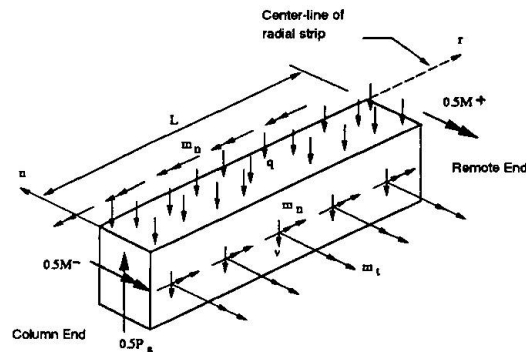


Fig. 3: Radial Half-Strip

The combination of shear and torsion on the side face of the radial half-strip is replaced by a statically equivalent line load,  $\bar{v}$ , acting on the strip. The term  $\bar{v}$ , referred to as the Kirchhoff shear, has its origins in elastic plate theory as a way of satisfying equilibrium at a free or simply supported edge of a plate.

$$\bar{v} = \frac{\partial m_n}{\partial n} + 2 \times \frac{\partial m_t}{\partial r} \quad [2]$$

The Kirchhoff shear has two components. The first is a shear resulting from the gradient in bending moment perpendicular to the radial strip. This is referred to as **primary shear**. The second is a shear resulting from twisting moment gradient along the side face of the radial strip, called **torsional shear**.

**Primary shear** results from the gradient in bending moment perpendicular to the radial strip. If bending moment gradient perpendicular to the radial strip is the result of beam action alone, then:

$$\frac{\partial m_n}{\partial n} = \frac{jd}{s} \times F_b' = \tau \times jd \quad [3]$$

where  $F_b'$  is the force gradient in the reinforcing bars perpendicular to the radial strip,  $s$  is the spacing and  $jd$  is the flexural moment arm. If  $F_b'$  is averaged over the bar spacing, the resulting term is the horizontal shear stress required for moment gradient,  $\tau$ .

In a region dominated by beam action, a limiting value of force gradient in the reinforcement is the equivalent of a limiting shear stress. Any limit to the force gradient that can be sustained at the boundary between steel and concrete is a bond limitation on the quantity  $\partial m_n / \partial n$ . Alternatively, for very lightly reinforced plate-column connections, force gradient at the edge of the radial strip may be limited by the spread of yielding.



**Torsional shear** is the result of gradient in the torsional moment on the side face of the radial strip, in a direction parallel to the radial strip. The factors governing the magnitude of the torsional moment and the torsional moment gradient are not known, nor is it clear how these quantities might be measured. However, it is possible to outline some of the effects of torsional shear on the basis of equilibrium conditions.

For a concentrically loaded column, the torsional moment must approach zero at the column support as a result of symmetry. Because of the way the radial strip is defined, the magnitude of the torsional moment at the remote end must also be zero, either by symmetry or boundary condition. Since the torsional moment is zero at both ends of the radial strip, the total contribution to Kirchhoff shear made by torsional moment gradient must be zero. Hence, torsional shear affects only the distribution of Kirchhoff shear along the length of the radial strip, leaving primary shear as the root source of all shear load on the side face of a radial strip. The effective centroid of the shear load is moved closer to the column by the action of torsional shear.

Fig. 4 shows a radial half-strip of an interior slab-column connection, excluding the bending moments about the  $n$ -axis, with the torsions and shears on the side faces replaced by the Kirchhoff shear. The term  $\bar{q}$  is a line load equivalent to the directly applied load,  $q$ . The radial strip supports all the loads by acting as a cantilever beam. The total flexural strength of the cantilever is the sum of  $M^-$  and  $M^+$ . Flexural equilibrium of the radial strip leads to Eq. 4 and vertical equilibrium produces Eq. 5. In each equation, the factor two accounts for the fact that both  $\bar{v}$  and  $\bar{q}$  are defined for a radial half-strip. The quantity  $P_s$  is the total load carried by one radial strip of an interior column-slab connection.

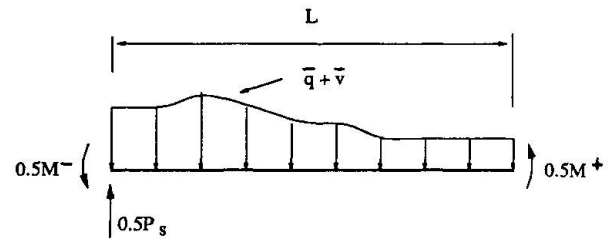


Fig. 4 Loading of Radial Half-Strip

$$M^+ + M^- = M_s = 2 \times \int_0^L (\bar{v} + \bar{q})r dr \quad [4]$$

$$P_s = 2 \times \int_0^L (\bar{v} + \bar{q})dr \quad [5]$$

Expressions for the negative moment capacity,  $M^-$ , at the column end of the strip and the positive moment capacity,  $M^+$ , at the remote end of the strip, are given in Eq. 6.

$$M^- = \rho^- \times f_y j d^2 \times c_2 \quad M^+ = k_r \times \rho^+ \times f_y j d^2 \times c_2 \quad [6]$$

The factor,  $k_r$ , accounts for the proportion of bottom steel that can be developed by the rotational restraint provided at the remote end of the radial strip. It is reasonable to assume that any steel which passes through the column contributes to  $M_s$ . There is, however, a problem in dealing with reinforcing bars which are close to the column. Furthermore, for uniformly spaced reinforcement, the values of  $\rho^-$  and  $\rho^+$  should not depend on whether the mat is bar centered or space centered. These problems are overcome by defining  $\rho^-$  and  $\rho^+$  as:

$$\rho^- = \frac{A_{sT}}{b \times d} \quad \rho^+ = \frac{A_{sB}}{b \times d} \quad [7]$$

$A_{sT}$  and  $A_{sB}$  are the total cross-sectional area of top and bottom steel, respectively, passing through the column plus one half the area of the first top or bottom bar on either side of the column. The term  $b$  is the column dimension plus the distance to the first reinforcing bar on either side of the column.

To evaluate the integrals of Eqs. 4 and 5, assumptions are made regarding the distribution of line load along the length of the radial strip. These assumptions both simplify and optimize the loading of the radial strip in a manner generally consistent with a lower bound approach.

- All Kirchhoff shear is assumed to be the result of primary shear. The torsional shear contribution is considered negligible because the deformations of a plate-column connection that fails in brittle punching are not consistent with the development of large torsional moments.
- At a distance  $l$  from the column end of the radial strip, the Kirchhoff shear decreases from the maximum value permitted by primary shear ( $(\partial m_n / \partial n)_{\max}$ ) to a value of zero. The length  $l$  is referred to as the loaded length of the radial strip.
- The direct load on the radial strip is assumed small compared to  $\bar{v}$  and is neglected ( $\bar{q} = 0$ ).

Based on these assumptions, the optimized loading of a radial half-strip is shown in Fig. 5. The loading term  $w$  is defined as:

$$w = \left( \frac{\partial m_n}{\partial n} \right)_{\max} = F_b'_{\max} \times \frac{jd}{s} = \tau_{\max} \times jd \quad [8]$$

It is convenient to consider  $w$  as the simplified, optimized Kirchhoff shear load acting on one side of a radial strip by an adjacent quadrant of two-way plate. Because a radial strip of an interior column-slab connection has two adjacent quadrants of two-way plate, the total line load on a radial strip of an interior column-slab connection is  $2w$ . For an edge or corner column, however, there will be radial strips that are parallel to the free edge of the plate and have only one adjacent quadrant of two-way plate. For these strips, the total line load is  $w$ .

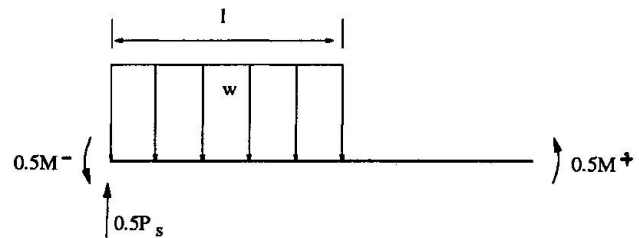


Fig. 5 Simplified Loading of Radial Half-Strip

Eq. 8 suggests that  $w$  may be based on either the maximum force gradient,  $F_b'_{\max}$ , in the reinforcement perpendicular to the radial strip or a maximum critical shear stress,  $\tau_{\max}$ , applied on the side faces of the radial strips.  $F_b'_{\max}$  may be obtained from an estimate of the bond strength as governed by splitting failure.  $\tau_{\max}$  may be obtained from the critical value of shear stress as defined by building codes for one-way flexural members. Since most treatments of splitting bond failure focus on either lap splices or anchorage zones rather than locations at some distance from the ends of the bars,  $\tau_{\max}$  provides a more attractive basis for a predictive model for punching shear.

For simplicity, building codes usually replace  $\tau_{\max} \times j$  with  $v_c$ . The critical value of  $v_c$  according to the ACI Standard<sup>4</sup> and the corresponding value of  $w$  are:

$$v_c = 0.166 \times \sqrt{f'_c} \quad w_{ACI} = d \times 0.166 \times \sqrt{f'_c} \quad [9]$$

The assumptions made regarding the distribution of line load along the length of a radial strip and the method chosen for estimating  $w$  result in the simplified free body diagram shown in Fig. 5. Using this figure, Eq. 4 may be rewritten and solved for  $l$  as follows:

$$M_s = 2 \times \int_0^L (w)r dr = 2 \times \int_0^l (w)r dr = 2 \times \frac{wl^2}{2} \quad ; \quad l = \sqrt{M_s/w} \quad [10]$$

Substituting  $l$  into Eq. 5 yields:

$$P_s = 2 \times \int_0^L (w)dr = 2 \times \int_0^l (w)dr = 2 \times wl = 2 \times \sqrt{M_s \times w} \quad [11]$$

The punching capacity of a slab-column connection is obtained by summing the contribution of each radial strip.



### 3 Discussion

The bond model, using  $w_{ACI}$ , was applied to 115 tests reported in the literature. The ratios of test load to predicted load are shown in Fig. 5. The average ratio of test to predicted punching load is 1.29 with a coefficient of variation of 12.3 per cent. Using the ACI<sup>4</sup> and BS 8110<sup>5</sup> code procedures on the same body of data, the average test to predicted values are 1.59 and 1.06 and the coefficients of variation are 26.5 and 15.1 per cent, respectively.

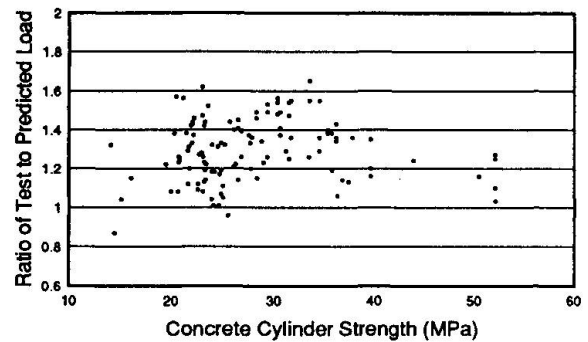


Fig. 6 Comparison of Test Results with Bond Model Predictions

The difference between the average test to predicted ratio for the ACI and BS 8110 codes can be attributed to differing design philosophies. The quality of these models should be judged on the consistency of their predictions rather than the magnitude of the average test to predicted ratio, since this can be adjusted simply by multiplying by a constant.

It is considered that the principal reason for the bond model consistently underestimating punching strengths is that the contribution of torsional shear is neglected. Despite this approximation, the bond model produces results that are more reliable than most building codes currently in use. Furthermore, the model is simple to apply and does not resort to the definition of artificial critical sections for shear.

The curved arch of the bond model is a natural progression from the straight-line compression strut of the truss model. In this way, the bond model is consistent with the truss model. The curvature of the arch requires a tension field within the concrete. The magnitude of this tension field is governed indirectly by the beam action shear perpendicular to the arch. As shown above, beam action shear as limited by bond can be represented as a critical shear stress. Thus, the bond model shows why the code approaches for estimating punching strength based on a critical shear stress acting on a critical shear section give satisfactory results.

The bond model links shear strength and bond strength at locations other than anchorage or splice locations. The importance of bond in the vicinity of the column has not been fully appreciated. The link between force gradient in the reinforcement and punching strength also explains why excessive yielding of the reinforcement in the vicinity of the column produces lower punching strengths.

### 4 References

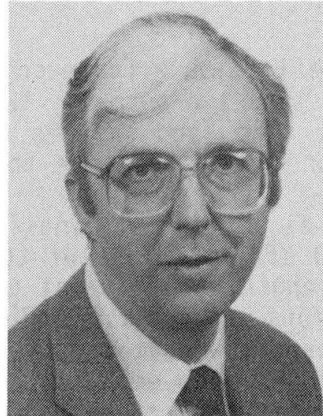
- 1 ALEXANDER, S.D.B., and SIMMONDS, S.H. 1987. Ultimate strength of slab-column connections. *American Concrete Institute Structural Journal*, Vol.84, No.3, pp. 255-261.
- 2 ALEXANDER, S.D.B. 1990. Bond model for strength of slab-column joints. Ph.D. thesis. Department of Civil Engineering, University of Alberta.
- 3 KINNUNEN, S., and NYLANDER, H. 1960. Punching of concrete slabs without shear reinforcement. *Transactions of the Royal Institute of Technology (Sweden)*, No.158, Stockholm, pp. 1-110.
- 4 ACI COMMITTEE 318-89: 1989 Building code requirements for reinforced concrete. American Concrete Institute, Detroit, MI.
- 5 BRITISH STANDARDS INSTITUTION, 1985. The structural use of concrete: Part 1, Code of practice for design and construction (BS 8110:Part 1). British Standards Institution, London.

## Design of Slab-Column Frames

### Conception de cadres dalles-colonnes

### Entwurf von Stahlbeton-Plattenträger-Strukturen

**James R. CAGLEY**  
President  
Cagley & Associates  
Rockville, MD, USA



James R. Cagley is a fellow of the ACI and has served on the ACI 318 Standard Building Code Committee since 1973. He is registered in 32 states in the USA and has practiced in many other countries.

#### SUMMARY

In the last 10 years a significant number of slab-column frame structures have been designed and constructed in the Washington D.C. area. Flat plate construction has been very popular for many years in Washington because of the stringent building height limitations caused by a desire not to overshadow the nation's Capitol building. The use of slab-column frames allows a 10-story office building with a total height limitation of approximately 32 m. Elimination of exterior masonry walls and interior masonry partitions led designers to look for other methods of resisting wind loads. Hence, the development of the slab-column frame.

#### RÉSUMÉ

Dans les 10 dernières années, un nombre important de structures en cadres dalles colonnes ont été dimensionnées puis réalisées dans les environs de Washington DC, USA. La construction de bâtiments relativement plats a été très répandue depuis de nombreuses années du fait des restrictions impératives sur la hauteur des édifices en vue d'éviter qu'ils ne dominent le Capitole lui-même. C'est ainsi que l'utilisation des structures en cadre dalles-colonnes permet de construire des immeubles de bureaux de 10 étages, dont la hauteur n'excède pas 32.00 m. L'élimination des parois extérieures et des galandages en maçonnerie a nécessité la recherche d'autres méthodes pour contreventer les bâtiments, d'où le développement de l'étude des cadres dalles-colonnes.

#### ZUSAMMENFASSUNG

In den letzten 10 Jahren wurden in Washington, DC viele Flachdecken entworfen und gebaut. Flachdecken waren in Washington auf Grund der Höhenbeschränkung für Gebäude, um das Kapitol nicht zu beschatten, für viele Jahre weit verbreitet. Die Verwendung dieser Bauweise machte es möglich, ein zehngeschossiges Bürogebäude mit einer Gesamthöhe von etwa 32 Metern zu errichten. Durch das Weglassen von Aussen- und Innentragwänden waren die Entwerfer gezwungen, die Rahmenwirkung mit den Stützen heranzuziehen.



## 1. INTRODUCTION

In the last 10 years a significant number of slab-column frame structures have been designed and constructed in the Washington, D.C. area. Flat plate construction has been very popular for many years in Washington because of the stringent building height limitations caused by a desire to not overshadow the nation's capitol building. The use of slab column frames allows for the construction of a 10 story office building with a total height limitation of approximately 105'. Elimination of substantial exterior masonry walls and interior masonry partitions caused designers to look for other methods of resisting wind loads. Hence, the development of the slab-column frame.

A slab-column frame is by definition a frame composed of slabs and columns in lieu of beams and columns. The slabs are normally two-way systems such as flat plates, flat slabs, waffle slabs or slab band systems. The purpose of using these types of systems is basically economy and a desire to avoid the use of shear walls.

In many building types such as office buildings, the use of shear walls causes many impediments to planning and efficient use of the floor space. If the core areas provide enough shear wall length, this is not a problem but often that is not the case and supplemental locations must be used. The economy of cast in place concrete construction is greatly enhanced when the only formwork which is required is flat deck forming and column forming with emphasis on keeping columns the same size as much as possible. The formwork cost increases significantly with the addition of concrete beams and shear walls. As a result it has been proven to be quite economical to use slab-column frames as the systems for buildings of moderate height (up to 12-14 levels) and in areas of low seismic risk.

This type of system works very well in hotel room towers as it does for office buildings. Some of the same reasons such as a desire to maintain a minimal floor to floor height make the slab-column frame an ideal solution for hotel towers up to approximately 12 floors. The normal gravity load system is a post tensioned flat plate with a thickness of 6 1/2" or 7". When the moment transfer requirements in the slab at the lower floors become a very large magnitude it is necessary to go to another lateral load resisting system. Normally this would occur at around 12 levels and would require the use of a shear wall system for heights greater than that.

## 2. DESIGN BASIS

### 2.1 Gravity Load Design

The gravity load design of slab-column frames is commonly accomplished utilizing the equivalent frame method or some PC based software. PCA's ADOSS is the program commonly used for mild reinforced systems and our office uses the post tensioning program developed and marketed by Structural Data, Inc. for the design of post tensioned floor systems. The normal procedure is to design the floor system for gravity loads and then to check it for the combination of lateral loads and gravity loads. In most cases this will require the addition of small amounts of bonded reinforcing which should be concentrated in the area over the column and immediately adjacent to each side of the column.

### 2.1 Lateral Load Design

Although the gravity load design of slab-column frames is similar to other systems, the design for lateral loads places some added constraints on the designer. The slab-column frame is a very flexible system so that drift or lateral deflections are of primary importance. The calculation of lateral deflections are greatly affected by the assumptions.



Our office practice is as follows:

1. All buildings are designed for strength as per the appropriate building code. This is normally the Building Officials & Code Administrators (BOCA Code) in the Washington, D.C. area. The design wind speed is generally 80 or 90 mph.
2. The normal criteria which we use for wind drift is  $h/500$  or  $h/400$  where  $h$  is the height of the building under design. THIS IS NOT A CODE REQUIREMENT.
3. The wind load used for drift calculations is related to the highest recorded wind speed in the area. In the Washington area we would generally use 60 mph for our drift calculations. Our theory is that in most buildings discomfort due to movement should be avoided for normal or probable loadings. These are not necessarily the same as CODE loadings. It is easy to see that the calculated drift is less than half if 60 mph is used in lieu of 90 mph.
4. Reduced stiffnesses are used for the slab-column frames. The slab stiffness is based on 35% of the total bay width and the columns on 100% of their gross stiffness.
5. The lateral load analysis is accomplished with either ETABS, a program developed at the University of California and marketed by Computers & Structures, Inc., or one of several plane frame programs utilizing various modeling techniques.

A similar procedure is used for consideration of Zone 1 earthquake loadings. We are presently doing our first project in a Zone 2 area utilizing a slab-band system and the provisions of Chapter 21 in ACI 318-89 and the 1985 Uniform Building Code (UBC) allowing the use of two-way slab systems in zones of moderate seismic risk.

### 2.3 Column Design

Utilizing the information from the gravity load design of the slab system and the lateral load analysis of the slab-column frame our office uses a simplified moment magnification approach as proposed by MacGregor for medium height structures. A more exact method would be required for tall structures. This approach is valid when the stability index  $Q$  is between 0.0475 and 0.20.  $Q$  is defined as  $\sum P_u \Delta_1 / H_u h_u$ .  $P_u$  is the factored load of the entire story,  $\Delta_1$  is the first order story deflection.  $H_u$  is the total lateral load for this story and the stories above, and  $h_u$  is the unsupported clear height of the column.

The method is described in STABILITY ANALYSIS AND DESIGN OF CONCRETE FRAMES, James G. MacGregor and Sven E. Hage, ASCE Structural Journal, October 1977.

The structural magnified moments which will normally be significantly less than those utilizing the CODE equations are then combined as appropriate with the factored loads and moments from the gravity load analysis.

### 2.4 Shear Design

Typical two-way slab systems utilize a "shear cap" to increase the shear capacity of the slab system in the critical area surrounding the column and to allow the subsequent use of a thinner slab controlled by flexure and deflection considerations rather than shear.

The 1983 ACI 318 basically did not allow for the contribution of a column capital or bracket which lay outside a 45° tapered wedge. Consequently if the horizontal





extension of a "shear cap" was greater than the vertical depth of the "shear cap", the added horizontal concrete was of no value in calculating the shear capacity of the slab system. This meant that if a 4'-0" square "shear cap" that was 6" deeper than the slab was used with a 24" square column only the first 6" projection contributed to the shear capacity of the system and the second 6" projection did not affect the capacity. Obviously, this was not correct and a subsequent change in the 1989 CODE gives a basis for utilizing that capacity.

The 1989 ACI 318 requirement requires a gradual decrease in  $v_c$  from  $4/f'_c$  to  $2/f'_c$  as the ratio of the critical perimeter  $b_o$ , to the critical depth,  $d$ , increases. The requirement will mean that at the edge of a 4'-0" square "shear cap" with an 8" slab such as might be used on an office building, the allowable  $v_c$  would be  $3.32/f'_c$  in lieu of  $4/f'_c$  as might have been assumed for an interior column.

ACI-ASCE Committee 352 also has a recommendation in their "Tentative Recommendation for Design of Slab Column Connections in Monolithic Reinforced Concrete Structures". Their requirement is based on just two adjustments. If the ratio of the maximum perimeter of the slab critical section to slab effective depth is less than 20, the allowable  $v_c = 4/f'_c$ . If the value is between 20 and 40,  $v_c$  is modified to  $3/f'_c$  and if it is over 40  $v_c$  becomes  $2/f'_c$ . Our sample from above would have a ratio of  $4(48+d)$  over  $d$ . If we assume that  $d$  is 7 then  $212/7 = 30.3$  so  $v_c = 3/f'_c$ . Obviously, all of these values in any case would need to be adjusted as appropriate for other factors such as the aspect ratio of the column.

### 3. TEST PROGRAM

A small test program involving eight specimens was accomplished at the University of California at Berkeley in 1988 and '89 under the direction of Dr. Jack Moehle. The purpose of the program was to attempt to determine the effectiveness of a "shear cap" in increasing the shear capacity of a slab-column joint. The results of the testing were the confirmation of the allowable shear values indicated in both ACI-318-89 and the ACI-ASCE 352 report. The values are apparently conservative, but the failure mode is not as anticipated. The "shear caps" do not act as an extension of the column area but are much more flexible and actually tend to fall off the bottom of the slab. As previously noted, the allowables as proposed are appropriate.

### 4. DETAILING

Both the ACI-ASCE Committee 352 recommendations and the 1989 ACI 318 CODE require that some minimum amount of positive (bottom) reinforcing be continuous through the joint.

In slab-column frames there is often a requirement at the lower floors for continuous bottom reinforcing through the joint for strength considerations.

ACI-ASCE 352 and ACI 318-89 require some continuous bottom reinforcing in two-way slab systems at the supports regardless of the lateral load resisting system utilized for the building.

### 5. CONCLUSIONS

Slab-column frames have proved to be a viable, economical solution for many building projects in the Washington, D.C. area as well as other parts of the United States. In the last 3 or 4 years our office has designed at least 6 million square feet of construction utilizing this system. The system allows construction of large bay (30' x 30') or medium bay (20' x 20') office buildings with minimal floor to floor heights, since the effective structural depth is often no more than 8".

Although the system has limitations particularly for heavy seismic areas, it is a good solution for buildings in a concrete town like Washington, D.C. or any area of low-seismic risk.

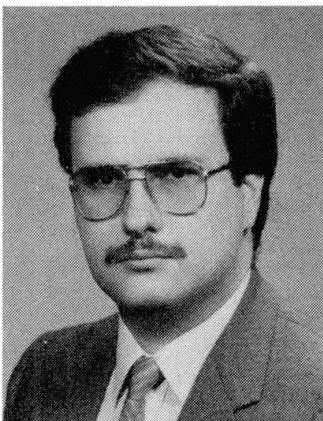
## Behaviour of Waffle Flat Slabs under Horizontal Load

Comportement des dalles nervurées soumises à des charges horizontales

Verhalten der Rippen-Flachdecken unter Horizontal-Belastung

### Valter J.G. LUCIO

Res. Assist.  
Techn. Univ.  
Lisbon, Portugal



Valter Lucio has been a research assistant at UTL Lisbon since 1980 and has been preparing his Ph.D. thesis on waffle slabs for the last 4 years, 3 of them at the PCL.

### Paul E. REGAN

Dr. Eng.  
Polytechn. Central London  
London, UK



Paul Regan has been at PCL since 1972 and has been active in research on flat slabs and particularly shear for many years.

### SUMMARY

This paper presents a model of the behaviour of column-supported slabs under lateral actions. A method is proposed for quantifying the rotational stiffness of slab-column connections for both solid and waffle slabs. The method takes account of the cracking of the slab. The results obtained from the model are compared with those from tests of reinforced concrete slabs.

### RÉSUMÉ

Cet article présente un modèle destiné à étudier le comportement de dalles sur colonnes soumises à des actions latérales. Une méthode est proposée afin de quantifier la rigidité de rotation des joints dalle-colonne pour des dalles pleines et nervurées tout en tenant compte de la fissuration des dalles. Les résultats du modèle sont comparés avec ceux provenant d'essais effectués sur des dalles en béton armé.

### ZUSAMMENFASSUNG

Der Artikel stellt ein Modell für das Tragverhalten von punktgestützten Platten unter Horizontal-lasten vor. Es wird ein Berechnungsverfahren für die Steifigkeiten des Stützen-Platten-Knotens bei Kassettendecken und massiven Decken vorgeschlagen. Dabei wird auf den Einfluss der Rissbildung unter Eigenlasten und Horizontallasten berücksichtigt. Die Berechnungsergebnisse wurden mit Versuchswerten verglichen.



## 1. INTRODUCTION

Equivalent frame methods offer an understandable and reasonable modelling of flat slab structures. In their usual forms they do however have problems in representing the behaviour of slab-column connections. These problems arise from geometry and from the effects of cracking.

## 2. EXPERIMENTAL STUDIES

Experimental data from realistic models subjected to lateral loading is available for tests by Lucio [1,2] on a waffle slab and by Long and Kirk [3] on solid slabs.

### 2.1 Waffle slab model

A column-supported waffle slab with 9 panels (Fig. 1) was tested at the Polytechnic of Central London. The slab, which represented typical prototypes to a scale of about 1 in 3.5, was supported on 16 columns and had solid infill panels with plan dimensions equal to  $3/8$  times the spans.

The slab was subjected to various levels of vertical and horizontal loading to study its behaviour under lateral load with different amounts of cracking caused primarily by uniform vertical loading. The rotations at the column heads and the reactions at their bases were measured with inclinometers and triaxial load cells [4]. The base measurements allowed the moments at the slab-column joints to be determined.

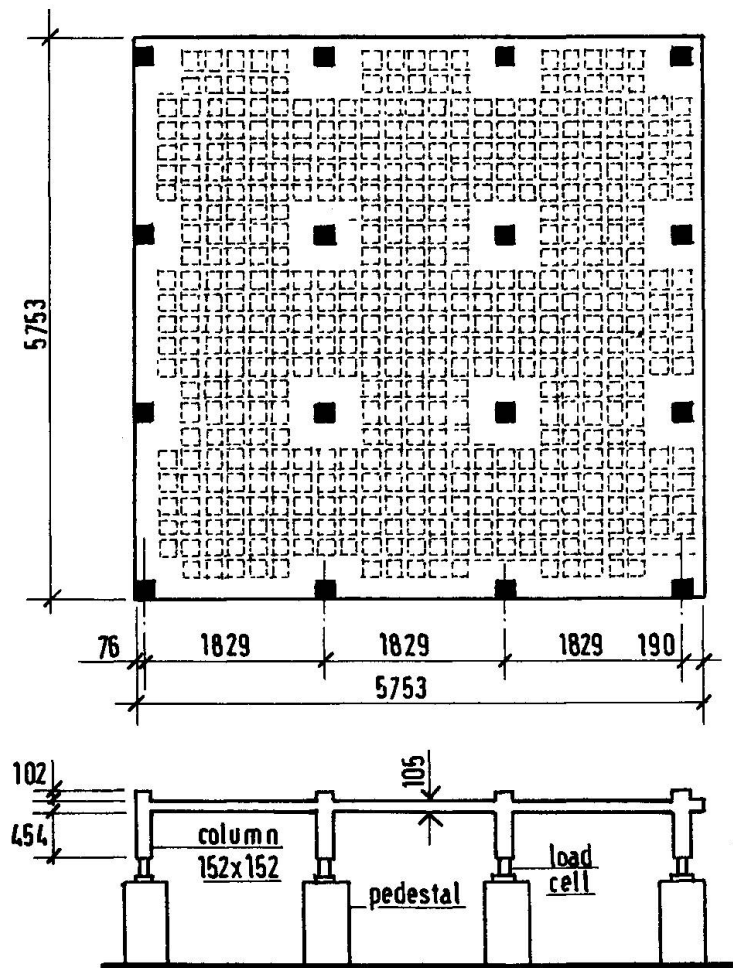


Fig. 1 Waffle slab tested by Lucio

Fig. 2 shows the rotations of an interior column head as functions of lateral load for various levels of prior vertical loading. The vertical loads during the lateral load tests were about 0.8 times the previous maxima.

Table 1 gives the stiffnesses of the structure at maximum horizontal loads in terms of  $H/a$ , where  $H$  is the total horizontal load and  $a$  is the lateral displacement at the level of the slab.

Prior Vert. Load (kN/m <sup>2</sup> )	H (kN)	H/a (kN/mm)
9.4	40	176
12.0	50	147
17.0	80	97

Table 1. Stiffness from lateral load tests

### 2.2 Solid slab models

Long and Kirk tested three models representing parts of flat slab structures (Fig. 3). The supports were two columns and one line support. The long edges of the models represented mid-panel lines and rotations at and normal to these edges were prevented by the application of moments.

Model 2 included an edge beam and is not considered here. The other two differed in terms of column dimensions. For slab 1, the edge column was 100 x 150mm and the internal column was 150mm square. In model 3 the corresponding dimensions were 150 x 225mm and 225mm square.

Displacements of 3mm were applied at the tops of the columns and horizontal reactions were measured at their bases. During horizontal loading, the vertical load represented the dead load of a prototype 3 times the model size, but the slabs had been preloaded to the prototype service load.

## 3. FRAME ANALYSIS

### 3.1 General

Equivalent frame methods for the analysis of flat slabs include those of ACI 318-89 [5], BS 8110 [6] and the flexible joint method (FJM) proposed by Regan [7]. In the code methods, vertical and horizontal loadings are treated by different models. For vertical loading the properties of the members may be directly those of the structure, ie.  $I = bh^3/12$  [6], in which case no allowance is made for the flexibility of the connections. Alternatively the column stiffnesses may be reduced to take account of this flexibility [5]. For horizontal loading the slab stiffness is reduced by considering an effective

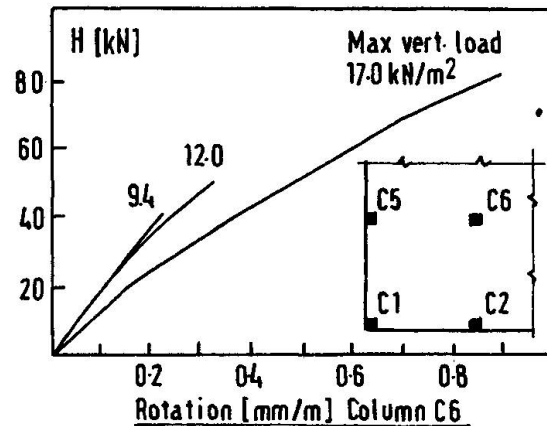


Fig. 2 Results of lateral load tests

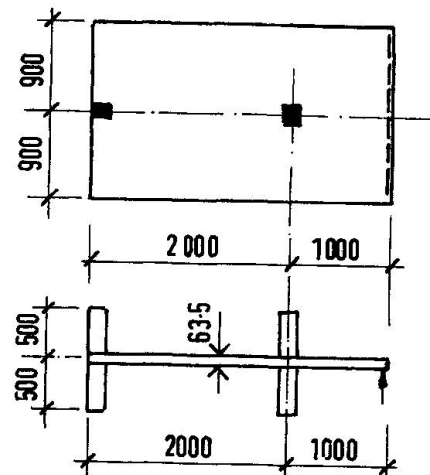


Fig. 3 Models of Long and Kirk



breadth less than the full width between panel centre lines.

The FJM uses a torsional spring (Fig. 4c) to simulate the flexibility of a slab-column joint. This allows the same model to be used for any loading. All three methods are based on uncracked elastic theory.

3.2 Elastic behaviour

If the column of Fig. 4a has the same stiffness as the wall of Fig. 4b and the slabs are similar, the application of equal moments will produce a greater rotation in the former case. For elastic conditions the stiffnesses ( $M/\theta$ ) for both cases can be calculated by the Finite Element Method. The results depend somewhat on details but published data [8-11] for solid slabs is quite consistent.

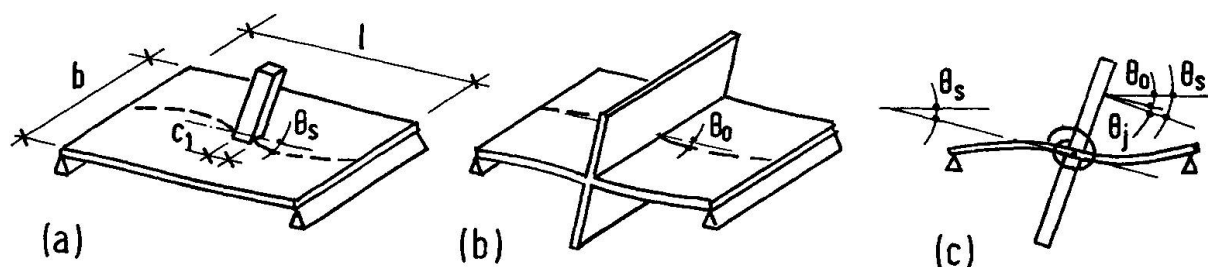


Fig. 4 Models for horizontal loading

The data can be presented in a form in which the slab rotation  $\theta_s$  of Fig. 4a is the sum of  $\theta_o$  (Fig. 4b) and a joint rotation  $\theta_j$ . Each rotation is equal to the applied moment divided by the relevant stiffness ( $K_s, K_o, K_j$ ).

$$\theta_s = \theta_o + \theta_j \quad \dots\dots(1)$$

$$\frac{1}{K_s} = \frac{1}{K_o} + \frac{1}{K_j} \quad \dots\dots(2)$$

where  $K_o/D = 12(b/l) (1-c_1/l)^{-3}$  and  $D$  is the flexural stiffness per unit width of slab.

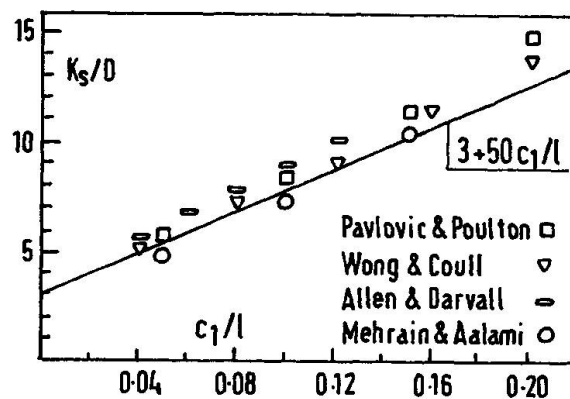


Fig. 5 Comparison of eqn. (3) with FEM results

Fig. 5 shows that FEM results for square columns ( $c_1 = c_2$ ) and square panels ( $b=l$ ) can be approximated by  $K_s/D = 3 + 50(c_1/l) \quad \dots\dots(3)$

Moderate variations of  $c_1/c_2$  have little effect on stiffness. Expression (3) can be used directly for square panels. For rectangular ones  $K_j$  can be calculated from equation (2) and combined with the appropriate  $K_o$ .

Fig. 6 shows the model used to analyse waffle slabs by the Finite Element Method. For the coffers available on the market, the

ratio between the flexural stiffnesses of the solid and waffle zones varies only in the range from 3 to 4. Equation (4) is proposed [12] to approximate elastic analysis of square waffle slabs and Fig. 7 compares it with FEM results.

$$K_S/D = (6.25 + 50c_1/l) (l_s/l + b_{SS}/l)^{0.75} (b_s/l)^{0.25} \dots\dots(4)$$

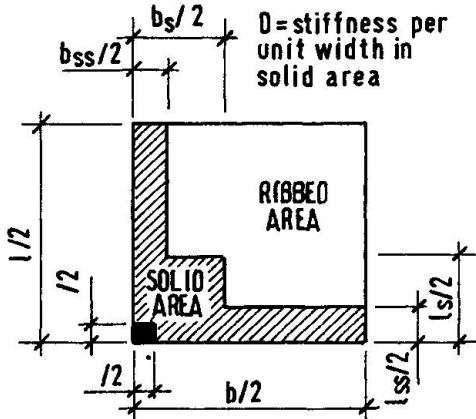


Fig. 6 Waffle slab model

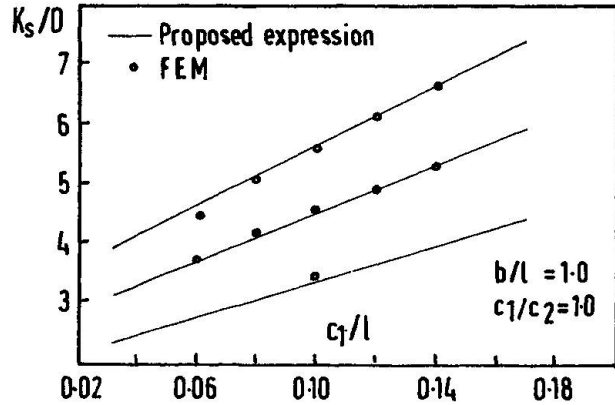


Fig. 7 Eqn. (4) compared with FEM data

### 3.3 Influence of cracking

The effect of vertical loading can be accounted for by a reduction of  $K_j$  to  $K_{jv}$ .

$$1/K_{jv} = \beta_1\beta_2 (m_{cr}/m)^2(1/K_j) + [1 - \beta_1\beta_2(m_{cr}/m)^2] [D/K_j D_{Cr}] \dots(5)$$

where  $\beta_1 = 1.0$  for high bond bars and 0.5 for plain bars and  $\beta_2 = 1.0$  for first loading and 0.5 for long term or repeated loading.  $m_{cr}$  is the cracking moment and  $m$  the applied moment at the column line and both of them may be averaged for the width of the column strip. For practical design the value of  $m$  should be that for the full service load. It is here taken as that for the maximum prior load.  $D$  is the uncracked and  $D_{Cr}$  the fully cracked (bare steel) stiffness again averaged for the width of the column strip.  $K_0$  can be taken to retain its uncracked value.

As shown in Fig. 2 the influence of horizontal loading itself is a further reduction of stiffness which can be accounted for by reducing  $K_{sv}$  to  $K_{sh}$  where

$$K_{sh} = K_{sv}/(1 + M/M_R) \dots\dots(6)$$

where  $M$  is moment acting between the column and the slab and  $M_R$  is the calculated resistance moment corresponding to flexural failure.

### 4. COMPARISON WITH TEST RESULTS

Table 2 presents the results of a comparison between the experimental stiffnesses of the three slabs discussed with values calculated by the method proposed. The agreement between the two sets of values can be seen to be very good.

Slab	H/a (kN/mm)	
	Test	Calc
Waffle	97	89
Long 1	1.66	1.66
Long 3	2.12	2.11

Table 2 Experimental and calculated stiffnesses



## 5. CONCLUSION

If the lateral load responses of flat slab structures are to be assessed realistically the models used in analysis must take account of the limited connections between the slabs and columns and also of the effects of cracking in the slabs.

There is no unique moment/rotation response for a slab-column connection as the local stiffness is greatly influenced by cracking produced by vertical loading, even if this involves no transfer of moment between the slab and column.

The model proposed provides a method of estimating joint stiffnesses and thence slab and column rotations, by accounting for geometric factors within an elastic approach and then modifying the results to allow for cracking.

## REFERENCES

- [1] Lucio V.J.G., An experimental model of a waffle slab with 9 panels, CREST Report Ai10, Lisbon, March 1990.
- [2] Lucio V.J.G., Description of the test of a waffle slab model with 9 panels, CREST Report Ai11, Lisbon, March 1990.
- [3] Long A.E. and Kirk D.W., Lateral load stiffness of slab-column structures, Reinforced Concrete Structures Subjected to Wind and Earthquake Forces, ACI Publication SP-63, Detroit 1980, pp 197-220
- [4] Lucio V.J.G. and Regan P.E., Triaxial load cells for the tests of a waffle slab supported by 16 columns, 9th International Conference on Experimental Mechanics, Copenhagen, 1990
- [5] ACI 318-89, Building code requirements for reinforced concrete, American Concrete Institute, Detroit, 1989
- [6] BS8110 - Structural use of concrete, British Standards Institution, London 1985.
- [7] Regan P.E., Behaviour of reinforced concrete flat slabs, Construction Industry Research and Information Association, Report 89, Feb. 1981
- [8] Wong Y.C. and Coull A., Effective slab stiffness in flat plate structures, Proc. Inst. Civil Engrs. Part 2, 68. Sept 1980 pp 721-735.
- [9] Allen F. and Darvall P. Lateral load equivalent frame, ACI Journal, No. 74-32, July 1977 pp 294-299
- [10] Pavlovic M.N. and Poulton S.M., On the computation of slab effective widths, ASCE Journal of Structural Engineering, Vol. 111 No. 2, Feb 1985 pp 363-377.
- [11] Mehra M. and Aalami B., Rotational stiffness of concrete slabs, ACI Journal No. 71-29, Sept. 1974, pp 429-435
- [12] Lucio V.J.G. Frame analysis of column supported slab structures, with special regard to waffle slabs. CREST Report, Ai15, Lisbon 1990.